A Proposal for the Mg^{2+} Binding Site of P-Type Ion Motive ATPases and the Mechanism of Phosphoryl Group Transfer†

Vladimir N. Kasho, Martin Stengelin,‡ Irina N. Smirnova, and Larry D. Faller*

CURE: Digestive Diseases Research Center, Department of Medicine, University of California at Los Angeles School of Medicine, and Wadsworth Division, Department of Veterans Affairs Medical Center, West Los Angeles, California 90073

Received February 28, 1997; Revised Manuscript Received April 28, 1997⊗

ABSTRACT: Mutations of D586 in the DPPR sequence of sodium pump decrease the enzyme's affinity for inorganic phosphate [Farley R. A., Heart, E., Kabalin, M., Putnam, D., Wang, K., Kasho, V. N., and Faller, L. D. (1997) *Biochemistry 36*, 941−951]. Therefore, it was proposed that D586 coordinates the Mg^{2+} required for catalytic activity. This hypothesis is tested (1) by determining the substrate for catalysis of ^{18}O exchange between inorganic phosphate and water and (2) by comparing conserved amino acid sequences in P-type pumps with the primary structures of enzymes of known tertiary structure that catalyze phosphoryl group transfer. From the isotope exchange data, it is concluded that the Mg^{2+}-dependent and Na^+- and K^+-stimulated ATPase binds Mg^{2+} before inorganic phosphate. Sequence homology is demonstrated between the conserved DPPR and MV(I,L)TGD sequences of P-type pumps and two conserved adenylate kinase sequences that coordinate Mg^{2+} and/or bind nucleotide in the crystal structure of the yeast enzyme. A model for the Mg^{2+} site of P-type pumps and the mechanism of phosphoryl group transfer is proposed and tested by demonstrating that the conserved sequences are also structurally homologous.

It has been known since the discovery of sodium pump that Mg^{2+} is required for enzymatic activity (*1*). Therefore, it is remarkable that the divalent cation is not even mentioned once in a recent book on structure−function relationships in Na,K-ATPase[1] (*2*). None of the amino acids that coordinate Mg^{2+} have been identified, and little is known about the function of Mg^{2+} in catalysis.

There has been one attempt to predict the folding of a segment of the largest cytosolic domain of P-type ATPases (*3*) containing three conserved amino acid sequences that have been implicated in ATP binding (*4*). The proposed structure for the nucleotide binding site resembles ADK (*5*) and has been tested by site-directed mutagenesis of Ca-ATPase (*6*). No evidence for the predicted interaction of aspartic acid in the DPPR sequence with ATP was found, but it was concluded from experiments with ^{32}P-labeled ATP and P_i that changing this aspartic acid either prevents phosphorylation (D → E) or slows the conformational change from E_1P to E_2P (D → N).

Our recent study of the corresponding mutations in the DPPR sequence of Na,K-ATPase supports the former conclusion (*7*). The effects of changing D586 (sheep α1 numbering) on ouabain binding and the rate (v_{ex}) and partition coefficient (P_c) for catalysis of ^{18}O exchange between P_i and H_2O were measured. No ouabain binding or ^{18}O exchange could be detected when aspartic acid was changed to glutamic acid. When aspartic acid was changed to asparagine, (1) the ouabain dissociation constant increased nearly 100-fold, (2) v_{ex} measured in 2 mM P_i decreased roughly 100-fold, (3) the apparent K_m for P_i increased at least 15-fold, and (4) P_c decreased 10-fold compared to wild type. Unmeasurable ouabain binding or catalysis of ^{18}O exchange by D586E and all four of the observations with D586N are consistent with impaired P_i binding to the mutants. However, since P_i and solvent-accessible carboxyl groups would both be negatively charged at the pH of our experiments, we proposed that D586 coordinates the Mg^{2+} ion required for catalytic activity.

In support of our proposal, a ternary enzyme−divalent cation−substrate complex has been demonstrated by EPR and NMR measurements with Mn^{2+} substituted for Mg^{2+} (*8*). The estimated distance between Mn^{2+} and the phosphorus atom of the P_i analogue methylphosphonate when both are bound to Na,K-ATPase is 6.9 Å, consistent with formation of a second-sphere $E-Mn^{2+}-H_2O-CH_3PO_3^{2-}$ complex (*9*).

In apparent opposition to our proposal, two groups have concluded from the concentration dependence of "back door" phosphorylation that Mg^{2+} and P_i bind randomly to Na,K-ATPase. However, they disagreed about whether binding is anticooperative (*10*) or cooperative (*11*).

† This research was supported by Grant MCB9507018 from the National Science Foundation and by a Veterans Administration Merit Review Award.

‡ Present address: Department of Microbial Technology, Bristol-Myers Squibb Pharmaceutical Research Center, New Brunswick, New Jersey 08903.

⊗ Abstract published in *Advance ACS Abstracts,* June 15, 1997.

[1] Abbreviations: Na,K-ATPase, Mg^{2+}-dependent and Na^+- and K^+-stimulated ATPase (EC 3.6.1.37); Ca-ATPase, Ca^{2+}- and Mg^{2+}-dependent ATPase (EC 3.6.1.38); H,K-ATPase, Mg^{2+}-dependent, H^+-transporting, and K^+-stimulated ATPase (EC 3.6.1.36); ADK, adenylate kinase (EC 2.7.4.3); CK, casein kinase (EC 2.7.1); AXP, adenosine 5′-tri-(T), di-(D), or mono-(M) phosphate; Ap_5A, P_1,P_5-bis-(5′-adenosine) pentaphosphate; FITC, fluorescein 5′-isothiocyanate; Tris, tris(hydroxymethyl)aminomethane; HEPES, *N*-(2-hydroxyethyl)piperazine-*N*′-2-ethanesulfonic acid; P_i, inorganic phosphate; H_2O, water; EPR, electron paramagnetic resonance; NMR, nuclear magnetic resonance; GCMS, gas chromatograph−mass spectrometer; SIM, selected ion monitoring mode; AE, average isotope enrichment; PDB, Protein Data Bank; SR, sarcoplasmic reticulum; PM, plasma membrane; rmsd, root mean square deviation.

S0006-2960(97)00472-8 CCC: $14.00

In this paper, we report two tests of the hypothesis that D586 coordinates Mg^{2+} and forms a ternary complex with P_i in the active site of Na,K-ATPase. First, the order of Mg^{2+} and P_i binding is investigated by determining the substrate for catalysis of ^{18}O exchange between P_i and H_2O. Second, the sequence of Na,K-ATPase is compared with the sequence of ADK. The second test is based on the assumption that the protein architecture evolved to catalyze phosphoryl group transfer from ATP to AMP might also be utilized by P-type pumps because catalysis is coupled to transport by initially transferring the γ-phosphoryl group of ATP to the enzyme. Sequence homologies with two peptides containing functional groups that coordinate Mg^{2+} and/or bind AMP in the crystal structure of yeast ADK are reported. A model for the Mg^{2+} binding site of P-type ion motive ATPases and the mechanism of phosphoryl group transfer is proposed and initially tested by demonstrating structural homology between the conserved amino acid sequences.

EXPERIMENTAL PROCEDURES

Materials

Enzyme. The procedure developed by Jørgensen (*12*) was used to isolate and purify membranes containing Na,K-ATPase from pig kidneys. The amounts of protein in the membrane preparations were determined by the Lowry method (*13*), and the specific ATPase activities of the preparations were 15−20 μmol of P_i produced (mg of protein)$^{-1}$ min^{-1} at 37 °C.

Synthesis of ^{18}O-Enriched Substrates. Oxygen isotope-enriched P_i was synthesized by previously described methods (*14*). Briefly, ultrapure and dry PCl_5 is reacted with an excess of >99% ^{18}O-enriched H_2O, and [^{18}O]P_i is isolated from the reaction mixture by ion-exchange chromatography.

Chemicals. Ultrapure PCl_5 was purchased from Alpha Products and >99% ^{18}O-enriched H_2O from Icon. All other reagents were purchased from Sigma Chemical Co.

Methods

Measurement of ^{18}O Exchange between P_i and H_2O. The exchange reaction was started by addition of enzyme to 0.5 mL of a solution containing 97−99% ^{18}O-enriched P_i and K^+. The concentration of the latter was constant and nearly an order of magnitude larger than the biggest $K_{0.5}$ for K^+ estimated with parameters for the equilibrium between Na^+ and K^+ conformations in the presence of Mg^{2+} (*15*) and the equation derived for an equivalent site mechanism (*16*). The enzyme concentration and incubation time at 25 °C were chosen to give a final average ^{18}O enrichment (AE = $\sum_j P^{18}O_j{}^{16}O_{4-j}/4\sum P^{18}O_j{}^{16}O_{4-j}$, $0 \le j \le 4$) ranging from 40% to 80% so that significant amounts of all five isotopomers were formed. The reaction was quenched, and P_i was isolated by applying the reaction mixture to a column (0.5 × 4 cm) of Dowex AG 1-X4 (100−200 mesh, Cl^- form). After successive washes with 10 mL of H_2O (18 MΩ), the column was acidified with 3.5 mL of 30 mM HCl, and the phosphate was eluted with an additional 5 mL of 30 mM HCl (*14*). Approximately 95% of the phosphate was recovered, lyophilized, and converted into volatile triethyl phosphate by reacting with diazoethane (*17*). The product was analyzed on a polar capillary column with a Hewlett-Packard 5972A GCMS operated in the SIM mode. Masses 155−163 were measured and corrected for spillover from unprotonated diethyl phosphate.

Theory of ^{18}O Exchange. The mechanism of enzymatically catalyzed ^{18}O exchange between P_i and H_2O by P-type ion motive ATPases involves formation of a noncovalent enzyme−substrate complex (E·P) that is converted into a covalent, phosphorylated enzyme intermediate (E−P) as shown in eq 1 (*18*). Since the concentration of H_2O (55.6 M) does not change, it is incorporated into k_{-2} which becomes a pseudo-first-order rate constant (k'_{-2}). Depending upon the values of the rate constants, a phosphate molecule may exchange more than one oxygen atom via the second step in the reaction before it is released from the enzyme. Assuming the oxygen atoms of bound phosphate are equivalent in the transition state, a statistical distribution of phosphate isotopomers is generated as a function of time that depends upon the initial isotopomer distribution and two experimentally determinable parameters. The partition coefficient (P_c) is the probability of P_i entering into the exchange reaction.

$$\mathrm{E} + \mathrm{P} \underset{k_{-1}}{\overset{k_1}{\rightleftharpoons}} \mathrm{E{\cdot}P} \underset{k_{-2}}{\overset{k_2}{\rightleftharpoons}} \mathrm{E{-}P} + \mathrm{H_2O} \qquad (1)$$

$$P_c = k_2/(k_{-1} + k_2) \qquad (2)$$

The exchange rate (v_{ex}) is the rate at which unlabeled oxygen enters P_i.

$$v_{ex} = k'_{-2}[\mathrm{E{-}P}] \qquad (3)$$

Hackney (*19*) has derived equations for calculating the fraction of P_i containing from zero to four ^{18}O atoms as a function of time from the starting distribution of phosphate isotopomers. The first-order rate constant in these equations (k) is related to v_{ex} by eq 4 (*20*). Values for the initial exchange rate and partition coefficient were estimated by simultaneously fitting the equations for each of the five isotopomers to the observed isotopomer distributions with the SigmaPlot 5.0 curve-fit program and substituting the total (denoted by subscript o) P_i concentration into eq 4 ($[P^{18}O_4]_o \simeq [P_i]_o$, since AE > 97%).

$$kP_c[P^{18}O_4] = (1 - P_c)v_{ex} \qquad (4)$$

Molecular Modeling. Sequence searches of the SwissProt data base were carried out via the internet with BLASTP software (*21*). In reporting searches, letters in parentheses are used to indicate conservative amino acid substitutions (*4*) in a sequence; e.g., MI(V)TGDNK means that valine is sometimes found instead of isoleucine. Protein structures deposited in the Brookhaven PDB were modeled with a Pentium Pro 200 MHz computer and either RASMOL 2.6 (Glaxo Wellcome, U.K.) or CHEM3D (ChemOffice Pro 3.5) software. Allowed conformations of peptides were predicted by constructing the peptide and minimizing the energy with the CHEM3D algorithm. The peptide conformation reported is the minimum reached by beginning with the lowest energy conformations of the individual amino acids.

RESULTS

Dependence of Exchange Parameters on P_i and Mg^{2+} Concentrations. The exchange parameters estimated from

Table 1: Dependence of Exchange Parameters on $[P_i]_o$ and $[Mg^{2+}]_o$[a]

$[P_i]_o$ (mM)	$[Mg^{2+}]_o$ (mM)	enzyme preparation 1 v_{ex}[b]	1 P_c	2 v_{ex}	2 P_c	3 v_{ex}	3 P_c
0.34	0.34	0.87	0.201	1.60	0.244	1.38	0.283
0.37	1.04	2.67	0.245	2.99	0.227	2.60	0.250
0.46	3.46	4.99	0.301	5.18	0.227	5.11	0.292
0.72	10.39	7.18	0.293	7.25	0.248	6.84	0.245
1.04	0.37	3.32	0.225	4.09	0.223	3.10	0.220
1.12	1.12	6.35	0.222	7.33	0.227	6.48	0.247
1.39	3.69	9.38	0.271	11.44	0.247	9.44	0.241
1.61	34.28	8.06	0.253	10.05	0.226	9.09	0.254
2.18	11.18	11.93	0.264	14.71	0.240	13.23	0.238
3.43	0.46	7.40	0.246	9.67	0.221	8.71	0.226
3.69	1.39	11.65	0.261	14.53	0.236	12.76	0.245
4.58	4.58	14.48	0.274	18.51	0.237	16.13	0.244
4.88	36.88	12.99	0.262	17.67	0.248	15.92	0.250
7.18	13.88	16.66	0.287	21.12	0.256	18.82	0.267
10.4	0.65	13.32	0.263	16.83	0.245	14.09	0.262
11.2	2.18	16.25	0.272	21.01	0.251	18.98	0.253
13.9	7.18	19.69	0.291	24.71	0.270	20.27	0.283
16.1	45.81	18.85	0.299	24.81	0.285	21.78	0.306
21.8	21.76	21.76	0.284			22.94	0.299

[a] 10 μg mL^{-1} protein in 50 mM Tris-HCl at pH 7.4 and 25 °C containing 10 mM KCl, adjusted to 250 mM ionic strength with choline chloride. [b] μatom min^{-1} mg^{-1}.

measurements of the isotopomer distribution as a function of the total P_i and Mg^{2+} concentrations are reported in Table 1. No exchange of ^{18}O between P_i and H_2O could be measured ($v_{ex} = 0$) in the absence of Mg^{2+} or in the presence of ouabain, and there is no apparent trend of the P_c values in Table 1 with either Mg^{2+} or P_i concentration ($P_c = 0.255 \pm 0.025$, $n = 56$). The total concentrations of P_i were chosen to give an array of points (p, m) where $p = 0.33$, 1, 3.3, or 10 mM is the free P_i concentration and $m = 0.33$, 1, 3.3, 10, or 33 mM is the free Mg^{2+} concentration. A literature value of the MgP_i dissociation constant (8.5 ± 0.4 mM) for comparable experimental conditions (0.1 M HEPES−tetramethylammonium at pH 7.2 and 25 °C) was used in the calculation (*22*). Three different enzyme preparations were studied. Other details of the measurements are given in one of the footnotes (*a*) of the table.

Comparison with Known Structures. A BLASTP search for homologies with the DPPR sequence of sodium pump using a query sequence from sheep α1 confirmed that the sequence DPPR is conserved in P-type pumps (*4*) but did not produce any alignments with kinases of known three-dimensional structure. However, the sequence DGFPR was discovered by manually searching the yeast ADK primary structure. Conservation of this sequence in adenylate kinases from different species was confirmed by finding the sequence DGF(Y)PR in 31 of the 32 ADK primary structures in the SwissProt data base at the time of the search.

Figure 1 shows that the DGFPR sequence of ADK functions in both Mg^{2+} and nucleotide binding. The figure was drawn with the coordinates deposited in the Brookhaven PDB for yeast ADK in the closed conformation with Ap_5A and Mg^{2+} bound (*23*). In the crystal structure, D89 of the DGFPR sequence (green) forms a second-sphere coordination complex with Mg^{2+}, and R93 (behind) hydrogen bonds to the α-phosphate of the nucleotide in the AMP site. The divalent cation is not drawn to scale in order to show more

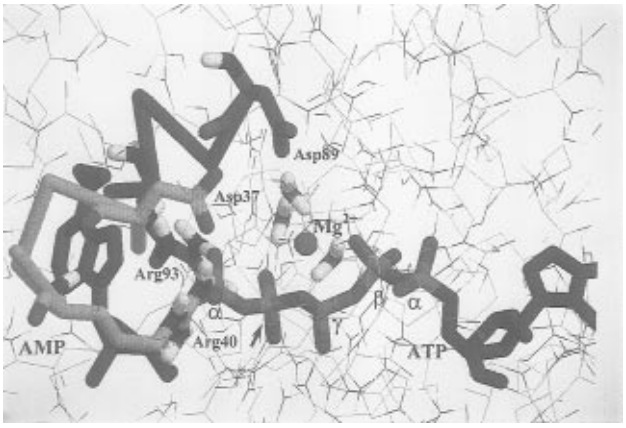

FIGURE 1: Mg^{2+} site of ADK. The closed conformation of yeast ADK with bound Ap_5A and Mg^{2+} generated from the coordinates deposited in the Brookhaven PDB with RASMOL software is shown. For clarity, some amino acids have been omitted, and only the DMLR (yellow) and DGFPR (green) sequences of the protein, Ap_5A, and the H_2O molecules in the primary coordination sphere of Mg^{2+} are represented by sticks. The arrow indicates the "extra" phosphate in Ap_5A.

Table 2: Comparison of $TGD(X)_yK(R)$ Sequences

enzyme	sequence	y	no. of examples
Na,K-ATPase	TGDHPITAK	5	19
H,K-ATPase	TGDHPITAK	5	4
PM Ca-ATPase	TGDNINTAR	5	7
PM Na-ATPase	TGDFVGTAR	5	2
PM H-ATPase	TGDAVGIAK(R)	5	3
ADK	T(S,A)GDM(L)L(M,F)R	2	32
PM K-ATPase	TGDNPK	2	1
PM K-ATPase	TGDNR	1	1
SR Ca-ATPase	TGDNK	1	14

clearly the three H_2O molecules in the primary coordination sphere of Mg^{2+}. Another arginine (R40) in the sequence TGDMLR (yellow, TG not shown) hydrogen bonds to the α-phosphate of the nucleotide in the AMP site from the other side (front), and the aspartic acid in this sequence (D37) is positioned so that it could act as another outer sphere ligand of the divalent cation.

There are two conserved TGD sequences in P-type pumps (*4*). One of them [MV(I,L)TGD] is positioned close to the α- and β-phosphates of ATP in the ADK-like fold predicted by Taylor and Green (*3*). The data base was searched to see if this sequence in pumps is followed by a positive charge like the TGD sequence of yeast ADK in Figure 1. Table 2 shows that there is remarkable conservation of the sequence $TGD(X)_yK(R)$, where X is an intervening amino acid and y may be 1, 2, or 5 depending upon the ion(s) transported and the source of the pump.

Figures 2 and 3 compare the DGFPR and TGDMLR conformations observed experimentally in the complex of yeast ADK with Ap_5A and Mg^{2+} (*23*) with the conformations of the sequences DPPR, TGDHPITAK, and TGDNK predicted by energy minimization. By rotating the structures 90° so that the polypeptide chains are perpendicular to the plane of the page (not shown), it can be seen that the positively (R or K) and negatively (D) charged groups emerge from the same side in a plane parallel to the backbone axis. The same scale was used for all of the structures in each figure so that the distances between the charged functional groups can be visually compared. The empirical

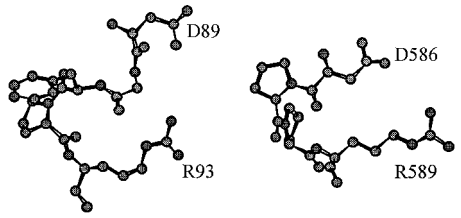

FIGURE 2: Comparison of DGFPR and DPPR conformations. The structure of DGFPR in the crystals of yeast ADK with Mg^{2+} and Ap_5A bound (left) is compared with the predicted structure of DPPR (right). The scale is the same for both polypeptides.

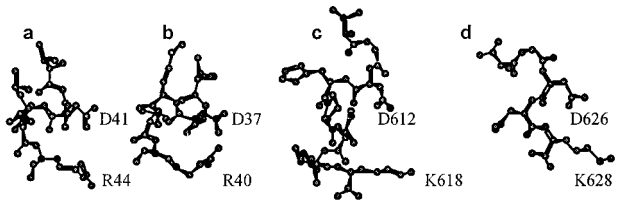

FIGURE 3: Comparison of $TGD(X)_yK(R)$ conformations. The structures of TGDLLR in pig ADK without bound ligands (a) and TGDMLR in yeast ADK cocrystallized with Mg^{2+} and Ap_5A (b) are compared with the predicted structures of TGDHPITAK (c) and TGDNK (d) polypeptides found in Na,K-ATPase and SR Ca-ATPase, respectively. All of the peptides are drawn to the same scale.

conformation of the TGDLLR sequence of pig ADK crystallized without added ligands is also shown in Figure 3.

DISCUSSION

No catalysis of ^{18}O exchange in the absence of Mg^{2+} confirms that a ternary complex of Mg^{2+}, P_i, and enzyme forms. A P_c value independent of either Mg^{2+} or P_i concentration indicates that ^{18}O exchange is catalyzed by a single mechanism.

Substrate for the Exchange Reaction. To learn whether the substrate is P_i or MgP_i and the order in which the reactants bind, equations were derived for alternative mechanisms and their predictions were compared with the empirical dependence of v_{ex} on the concentrations of Mg^{2+} and P_i. The mechanisms that were tested are shown in Table 3. It was assumed that ligand binding (double-headed arrows) is fast compared to phosphorylation of the enzyme in deriving the rate equations. All of the mechanisms predict hyperbolic dependence of v_{ex} on the free concentration of the independent variable (column 2). However, the expressions for the maximum exchange rate (V_{max}) in column 3 and the substrate concentration at half the maximum rate ($K_{0.5}$) in column 4 are different. K_2 is the equilibrium constant between the Michaelis complex and phosphorylated enzyme (e.g., $[E-MgP_i]/[E\cdot MgP_i]$ in mechanism 1). In the sequential mechanisms, the maximum rate is the rate constant for covalent bond formation (k_2) times the fraction of the enzyme with substrate attached that is unphosphorylated [$1/(1 + K_2)$], and $K_{0.5}$ is the substrate dissociation constant corrected for binding of the other ligand in the ternary complex times the fraction of enzyme with substrate bound in the Michaelis complex. An upper case K subscripted by the symbol for a substrate denotes the dissociation constant from a binary (unprimed) or ternary (primed) complex with the enzyme (e.g., K_P and K'_P in the table footnote). Since the product of the dissociation constants for the sequential steps in either of the parallel pathways to $MgE\cdot P$ in mechanism 5 must be the same ($[E][Mg^{2+}][P_i]/[MgE\cdot P]$), the effect of the first ligand bound on the affinity of the enzyme for the second ligand is independent of the order in which they bind and can be expressed by the ratio (α) of the dissociation constants of either ligand from the ternary and binary complexes with enzyme (table footnote).

The data in Table 1 are plotted against $[P_i]$, $[Mg^{2+}]$, and $[MgP_i]$ in Figure 4. The rates measured with different enzyme preparations have been normalized by fitting the Michaelis equation ($X = [P_i]$) to the individual data sets and plotting the ratio of v_{ex} to the estimate of V_{max}. The concentrations of free Mg^{2+}, P_i, and MgP_i (no subscript) were calculated with eq 5. This equation assumes that P_i forms a

$$[MgP_i]^2 - ([Mg^{2+}]_o + [P_i]_o + K_d)[MgP_i] + [Mg^{2+}]_o[P_i]_o = 0 \quad (5)$$

1:1 complex with Mg^{2+}. The MgP_i dissociation constant (K_d) was taken from the literature (Results).

Mechanisms 1, 3, and 4 can be rejected because they predict the wrong dependence of either V_{max} or $K_{0.5}$ on $[Mg^2]$ and/or $[P_i]$ when v_{ex} is plotted against the independent variable. In mechanism 1, the substrate is MgP_i, and the expression for $K_{0.5}$ in Table 3 is independent of the free Mg^{2+} or P_i concentration. However, Figure 4c shows that $K_{0.5}$ depends directly on $[Mg^{2+}]$ experimentally. Mechanism 3 assumes ordered binding of P_i and then Mg^{2+}. The equation for V_{max} in Table 3 is independent of free Mg^{2+} or P_i concentration, so plots of v_{ex}/V_{max} versus $[Mg^{2+}]$ should asymptotically approach 1 independent of $[P_i]$. Although the half-maximum Mg^{2+} concentration is clearly exceeded at all of the P_i concentrations in Figure 4b, the experimental data extrapolate to maximum v_{ex}/V_{max} values that depend directly on $[P_i]$. Mechanism 4 assumes two Mg^{2+} ions are required for catalysis of ^{18}O exchange. However, the predicted dependence of $K_{0.5}$ on $[Mg^{2+}]$ is inverse (Table 3), and the observed dependence of $K_{0.5}$ on $[Mg^{2+}]$ is direct (Figure 4c).

Mechanism 2 fits the data best (rmsd = 0.0045, $n - 3 = 53$). The lines in Figure 4 are simultaneous fits of the equation for mechanism 2 to all of the data in Table 1. Mechanism 2 assumes ordered binding of Mg^{2+} and then P_i. In this mechanism, P_i is the substrate. Mg^{2+} is a cofactor that binds to the enzyme and is required for P_i binding and enzymatic activity. The estimated Mg^{2+} dissociation constant from the enzyme (K_{Mg}) is 3.9 ± 0.3 mM, in good agreement with the value (2.8 ± 0.1 mM) obtained from stopped-flow studies of the rate of the conformational change in FITC-labeled enzyme for Mg^{2+} dissociation from the K^+ conformation (*15*).

Mechanism 5, which assumes Mg^{2+} and P_i bind randomly, cannot be ruled out (rmsd = 0.0048, $n - 5 = 51$). However, it is not surprising that mechanism 5 also fits the data satisfactorily because it includes mechanism 2 (upper pathway). A five-parameter fit of the equation for mechanism 5 to the data converges and gives an estimate of K_{Mg} (3.8 ± 0.5 mM) in good agreement with the estimate for the upper pathway alone. The estimates of the other parameters are not unique because of their interdependence. For example, K_P only appears in the equation for mechanism 5 multiplied by α. Therefore, fitting the equation for mechanism 5 with more parameters to the data is unjustified

Table 3: Mechanisms Tested[a]

mechanism	$v_{ex} = V_{max}[X]/([X] + K_{0.5})$ X	V_{max}	$K_{0.5}$
(1) $E \underset{K_{MgP}}{\longleftrightarrow} E{\cdot}MgP \underset{k'_{-2}}{\overset{k_2}{\rightleftharpoons}} E{-}MgP$	MgP_i	$k_2E_o/(1 + K_2)$	$K_{MgP}/(1 + K_2)$
(2) $E \underset{K_{Mg}}{\longleftrightarrow} MgE \underset{K'_P}{\longleftrightarrow} MgE{\cdot}P \underset{k'_{-2}}{\overset{k_2}{\rightleftharpoons}} MgE{-}P$	P_i	$k_2E_o/(1 + K_2)$	$[K'_P/(1 + K_2)](1 + K_{Mg}/[Mg^{2+}])$
(3) $E \underset{K_P}{\longleftrightarrow} E{\cdot}P \underset{K'_{Mg}}{\longleftrightarrow} MgE{\cdot}P \underset{k'_{-2}}{\overset{k_2}{\rightleftharpoons}} MgE{-}P$	Mg^{2+}	$k_2E_o/(1 + K_2)$	$[K'_{Mg}/(1 + K_2)](1 + K_P/[P_i])$
(4) $E \underset{K_{Mg}}{\longleftrightarrow} MgE \underset{K'_{MgP}}{\longleftrightarrow} MgE{\cdot}MgP \underset{k'_{-2}}{\overset{k_2}{\rightleftharpoons}} MgE{-}MgP$	MgP_i	$k_2E_o/(1 + K_2)$	$[K'_{MgP}/(1 + K_2)](1 + K_{Mg}/[Mg^{2+}])$
(5) 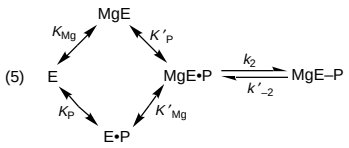	P_i	$k_2E_o/(1 + K_2 + \alpha K_{Mg}/[Mg^{2+}])$	$\alpha K_P[1 + K_{Mg}/[Mg^{2+}]]/(1 + K_2 + \alpha K_{Mg}/[Mg^{2+}])$

[a] X is the independent variable, $K_2 = k_2/k'_{-2}$, and $\alpha = K'_P/K_P = K'_{Mg}/K_{Mg}$, where $K_P = [E][P]/[E{\cdot}P]$ and $K'_P = [MgE][P]/[MgE{\cdot}P]$.

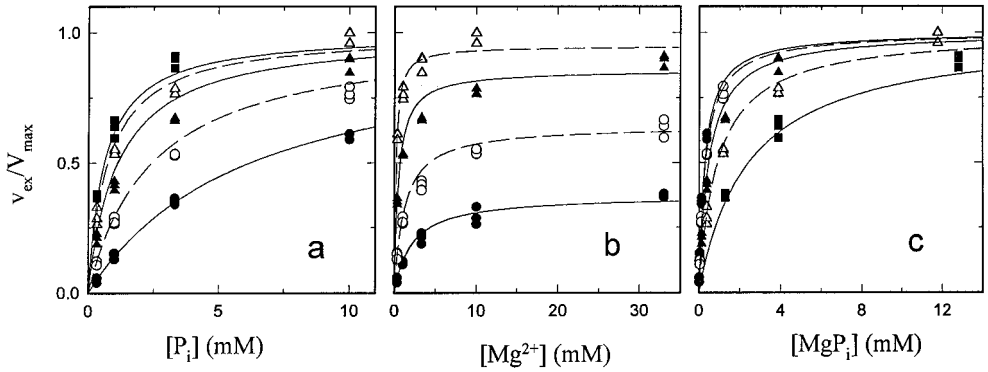

FIGURE 4: Concentration dependence of ^{18}O exchange between P_i and H_2O. The normalized exchange rates (v_{ex}/V_{max}) for three enzyme preparations are plotted against the free concentration of each of the possible substrates. The free concentrations of the fixed variable were 0.33 (●), 1 (○), 3.3 (▲), 10 (△), or 33 (■) mM Mg^{2+} (a, c) or P_i (b). The total concentrations of P_i and Mg^{2+} and the experimental conditions are reported in Table 1. The theoretical lines are a simultaneous fit of the equation for mechanism 2 in Table 3 to all of the data. Solid lines are drawn through solid symbols and dashed lines through open symbols for clarity.

mathematically. On the other hand, there is precedent for the estimates of K_2 and αK_P in the literature. Compared to back door phosphorylation in the presence of Mg^{2+} alone, K^+ reduces the amount of phosphoenzyme formed from [^{32}P]-P_i by about two-thirds with guinea pig kidney enzyme (*24*) and by about one-half with pig kidney enzyme (*25*). With the caveat that the P_i concentration used in these experiments (1 mM) may not have been saturating, the values of K_2 estimated by assuming that phosphorylation in the absence of K^+ is stoichiometric (0.5 and 1, respectively) bracket our estimate (0.59) from ^{18}O exchange data. The value of $K_{0.5}$ in 2 mM Mg^{2+} calculated from the estimate of K_2 and αK_P is 1.6 mM, in good agreement with the value of K_m(app) (1.5 ± 0.2 mM) estimated for wild-type Na,K-ATPase expressed in yeast cells (*7*). The value of K_p estimated from the ^{18}O exchange data is greater than 200 mM, suggesting that less than 2% of the reaction would go through the lower pathway in mechanism 5 if the free P_i and Mg^{2+} concentrations were equal.

In apparent contradiction to our conclusion that Mg^{2+} binds before P_i, all of the studies of back door phosphorylation of P-type ATPases in the literature claim that Mg^{2+} and P_i bind randomly. However, they are not in quantitative agreement. One study of Na,K-ATPase (*11*) concludes that P_i binds tighter to metalloenzyme (6.5-fold), and the other study of Na,K-ATPase (*10*) concludes that P_i binds tighter to holoenzyme (7.5-fold). In the case of Ca-ATPase, one study (*26*) concludes that Mg^{2+} and P_i have no effect on each other, and the other study (*27*) concludes that the ions bind with positive cooperativity (5-fold). One possible explanation of the different conclusions drawn from ^{18}O exchange and back door phosphorylation data is that only in the study by Punzengruber et al. (*27*) were the concentrations of free Mg^{2+} and P_i calculated and equations for alternative mechanisms subsequently derived and tested (*28*). Another possible explanation of the discrepancy is that the only metal present in the back door phosphorylation experiments was Mg^{2+}, whereas K^+ is also required for catalysis of ^{18}O exchange between P_i and H_2O by Na,K-ATPase (*29*) and there is evidence that the phosphoenzymes formed from P_i in the presence and absence of K^+ have different properties (*24*).

Deocclusion of K^+ by back door phosphorylation is a better reaction to compare with catalysis of ^{18}O exchange because the rates of both processes are proportional to the concentration of covalent phosphoenzyme with both Mg^{2+} and monovalent cations bound. Furthermore, the requirements for catalyzed exchange of ^{18}O between P_i and H_2O indicate that the phosphoenzyme formed from P_i and Mg^{2+} in the presence of K^+ is an intermediate in the hydrolysis of ATP (*29*), and an occluded K^+ form of dephosphoenzyme

is thought to be an intermediate in coupled cation transport (*30*). Forbush (*31*) has studied deocclusion of the K^+ congener Rb^+ by back door phosphorylation. Data for the rate of release of $^{86}Rb^+$ as a function of Mg^{2+} and P_i concentrations were fitted to a random binding mechanism with positive cooperativity (10−17-fold) between Mg^+ and P_i, and agreement with the back door phosphorylation experiments of Askari et al. (*11*) was claimed. However, neither Mg^{2+} binding to P_i nor simpler mechanisms were considered. When the data points that can be read from Figure 12 in the paper by Forbush (*31*) are analyzed as functions of the free Mg^{2+} and P_i concentrations, the equation for mechanism 2 fits the experimental results best. Fitting the equation for mechanism 5 with five parameters to the data is not justified mathematically but gives the same estimate of K_{Mg} (5.7 ± 1.6 mM) as mechanism 2 and suggests that even a smaller percentage of the reaction goes through the lower pathway than the analysis of the ^{18}O exchange data. Therefore, the published data of Forbush (*31*) for Rb^+ deocclusion by back door phosphorylation are also evidence for ordered binding of Mg^{2+} and then P_i to Na,K-ATPase.

Comparison with Known Structures. A superfamily of enolases was recently discovered by searching for conserved sequences in enzymes that catalyze reactions in which the first step is abstraction of a proton from the α-carbon of a carboxylic acid (*32*). The elementary reaction catalyzed by both P-type pumps and adenylate kinase is transfer of the γ phosphoryl group of ATP to another molecule. In the case of P-type pumps, the acceptor is the aspartic acid in the conserved sequence DK(R)TGTL(I)T (*4*) of the enzymes, and in the case of adenylate kinases, the acceptor is the phosphate of bound AMP. We have discovered a sequence in yeast ADK (DGFPR) that is homologous with the DPPR sequence of Na,K-ATPase. The sequence DPPR is conserved in P-type ATPases, and the sequence DGF(Y)PR is conserved in adenylate kinases. To explain reduced affinity for P_i when D586 in the DPPR sequence of Na,K-ATPase is mutated, we proposed that the carboxyl group coordinates Mg^{2+} (*7*). In support of this hypothesis, Figure 1 shows that D89 of the DGFPR sequence of yeast ADK forms a second coordination sphere complex with the Mg^{2+} required for ADK activity. In yeast ADK, the DGFPR sequence and another sequence TGDMLR reach around the bound AMP-like arms with the arginines (R93 and R40, respectively) holding the substrate in place by forming hydrogen bonds to the α-phosphate. Table 2 shows that both adenylate kinases and P-type pumps have a conserved sequence in which TGD is followed by a positive charge with one, two, or five intervening amino acids.

Proposal for the Mg^{2+} Site of P-Type ATPases. The amino acids that function as general bases in the abstraction of the proton from the α-carbon were identified by aligning the conserved sequences of members of the enolase superfamily (*32*). We propose that the DPPR and $TGD(X)_yK(R)$ sequences contribute to the Mg^{2+} and nucleotide binding site of P-type ATPases and function analogously to the homologous DGFPR and TGDMLR sequences in yeast ADK. For example, in sheep α1 Na,K-ATPase, D586 would correspond functionally to D89 of yeast ADK (Figure 1), R589 to R93, D612 to D37, and K618 to R40.

Substrate binding causes relative movement of the AMP and ATP domains of ADK from an open to a closed conformation of the enzyme (*33*). In yeast ADK cocrystallized with Ap_5A and Mg^{2+} (*23*), the donor (ATP) and acceptor (AMP) are aligned for phosphoryl group transfer via a pentacoordinate intermediate (*34*), and inversion of the configuration of the γ-phosphoryl group has been demonstrated in support of this mechanism (*35*). P-Type ATPases presumably catalyze phosphoryl group transfer by the same mechanism because the attacking nucleophile is a carboxyl group of the protein (*36*), pentacoordinate orthovanadate is a transition state analogue (*37*), and hydrolysis of ATP, which involves two transfers, occurs with retention of the stereochemistry of the γ-phosphoryl group (*38*). The AMP site of yeast ADK is better defined than the ATP site with five hydrogen bonds between the protein and the acceptor adenosine compared to only one between the protein and the donor adenosine (*23*). Since the acceptor is a protein residue in P-type pumps, we propose that the better defined nucleotide site of ADK is retained as the ATP site. Consistent with multiple contacts between the protein and ATP in P-type ATPases, changing arginine in the DPPR sequence of Ca-ATPase to methionine only reduced the rate of Ca^{2+} transport 40% (*6*). Conservation of the AMP site of ADK in P-type pumps is also consistent with our experimental evidence for negligible binding of P_i to sodium pump in the absence of Mg^{2+} because the positively charged amino acids that interact with the γ-phosphate of ATP bound to ADK are not in the AMP domain of the protein.

In the closed conformation of yeast ADK, Mg^{2+} is located near the β- and γ-phosphates of ATP and is thought to move with the phosphoryl group, which is transferred from the γ position in Figure 1 to the position occupied by the "extra" phosphate in Ap_5A (arrow). In addition to the three relatively fixed H_2O molecules shown coordinated to Mg^{2+}, there is a cluster of other H_2O molecules stabilized by interactions with the H_2O molecules in the metal's primary coordination sphere, the phosphates of Ap_5A, and groups on the protein including D37. We hypothesize that the aspartic acid in the $TGD(X)_yK(R)$ sequence of P-type ATPases is also involved in coordinating Mg^{2+} because changing aspartic acid to asparagine in the TGDNK and DPPR sequences of Ca-ATPase had similar effects on the Ca^{2+} transport rate (*6*). Third, instead of second coordination sphere bonding to Mg^{2+} could explain complete elimination of Ca^{2+} transport when aspartic acid is changed to bulkier glutamic acid in the DPPR sequence and retention of some activity (8%) when the same substitution is made in the TGDNK sequence. Retention of measurable ^{18}O exchange activity by the mutant D586N of Na,K-ATPase (*7*) is consistent with weaker but still significant bonding between divalent cations and amide groups. For example, an asparagine (N136) and a phosphate group from ATP are in the coordination sphere of Mg^{2+} in the crystal structure of CK cocrystallized with MgATP (*39*). This crystal structure also illustrates the feasibility of juxtaposing the DPPR and $TGD(X)_yK(R)$ sequences of P-type ATPases because an aspartate (D154) separated from N136 by approximately the same number of amino acids between the DPPR and $TGD(X)_yK(R)$ sequences of pumps is also close to Mg^{2+} in CK.

In the proposed model for P-type ATPases, the roles of the extra and β phosphates in Figure 1 are reversed. The extra phosphate becomes the β-phosphate of ATP, and the γ-phosphate is transferred to the β position in the figure.

Therefore, Mg^{2+} in the second coordination sphere of the aspartic acid in the DPPR sequence would be positioned between the β- and γ-phosphates of ATP bound to Na,K-ATPase, suggesting that Mg^{2+} enters the forward reaction complexed to ATP. There is kinetic evidence that Mg^{2+} remains bound after ADP dissociates from Ca-ATPase (*40*). In back door phosphorylation, Mg^{2+} is positioned to bind P_i and to accelerate phosphoryl group transfer by stabilizing the increased negative charge relative to the ground state on the oxygen atoms in the pentacoordinate transition state (*34*).

Tests of Hypothesis. The advantage of establishing structure−function relationships between enzymes that catalyze the same reaction is that they can be used to make predictions. For example, a second divalent cation binding site has been predicted for additional members of the enolase superfamily (*32*) because crystallographic studies have confirmed the biochemical evidence (*41*) that two Mg^{2+} ions are required for enolase catalytic activity (*42*). One prediction of the proposed model for the Mg^{2+} site of P-type ATPases is that the sequences conserved in pumps and adenylate kinases are also structurally homologous. This prediction was tested by molecular modeling followed by energy minimization. Figure 2 compares the DGFPR conformation observed experimentally in the complex of yeast ADK with Ap_5A and Mg^{2+} with the predicted conformation of DPPR. In both structures, the D and R groups point in the same direction and are approximately the same distance apart. The $TGD(X)_yK(R)$ sequence provides a more rigorous test of the model because the number of amino acids between the positively and negatively charged groups varies from one in SR Ca-ATPase to five in PM Ca-ATPase, the gastric H,K-ATPase, and Na,K-ATPase (Table 2). Figure 3 compares the observed conformations of the TGDLLR sequence in pig ADK without ligands and the TGDMLR sequence in yeast ADK cocrystallized with Ap_5A and Mg^{2+} with the predicted conformations of the peptides TGDHPITAK and TGDNK. The TGDNINTAR peptide found in PM Ca-ATPases essentially superimposes on the TGDHPITAK peptide of the Na,K- and H,K-ATPases (not shown). In the lowest energy conformations, the side chains with positively and negatively charged groups are on the same side of the polypeptide chain and lie in a plane parallel to the chain axis. A comparison of the empirical TGDLLR and TGDMLR structures indicates that Mg^{2+} and/or nucleotide binding induces a change in the conformation of the arginine side chain. Therefore, the positively charged side chain is flexible enough for the $TGD(X)_yK(R)$ sequences found in pumps to play the same functional role as the TGDMLR sequence despite the variable number of amino acids inserted between aspartic acid and arginine or lysine. The common feature of all the peptides in Figures 2 and 3 is that the positively and negatively charged side chains are arranged like the thumb and forefinger of a hand with sufficient flexibility to bind Mg^{2+} and/or ATP.

As an example of another testable prediction of the proposed model for the Mg^{2+} site of P-type ATPases, K_{Mg} should increase when aspartic acid is changed to asparagine in the DPPR sequence of Na,K-ATPase. This prediction can be checked in the future by obtaining an array of ^{18}O exchange data (Table 1) for the mutant D586N expressed in yeast cells and estimating K_{Mg} with the equation for mechanism 2 (Table 3).

Evolutionary Implications of Hypothesis. There is growing evidence that new enzymes originate by recruiting the chemistry evolved to catalyze an elementary reaction (*43*). Site-directed mutagenesis suggested a role for the aspartic acid in a conserved sequence of P-type pumps in binding Mg^{2+} that is supported by ordered binding of Mg^{2+} and then P_i to Na,K-ATPase and the discovery of a homologous sequence in adenylate kinases with the postulated function. Another sequence that binds Mg^{2+} and/or nucleotide in ADK is also conserved in P-type ATPases. Therefore, the Mg^{2+} site of yeast ADK (Figure 1) is proposed as a model for the Mg^{2+} site of P-type ion motive ATPases. Structural homology of the conserved peptides in pumps and adenylate kinases is demonstrated as an initial test of the model. The origin of P-type pumps is unknown (*4*). A corollary of the proposal in this paper for the Mg^{2+} site and mechanism of phosphoryl group transfer is that P-type pumps may have evolved by grafting part of the catalytic machinery of ADK for transferring phosphoryl groups onto an ion channel.

REFERENCES

1. Skou, J. C. (1957) *Biochim. Biophys. Acta 23*, 394−401.
2. Horisberger, J.-D. (1994) *The Na,K-ATPase: Structure−Function Relationship*, R. G. Landes Co., Austin, TX.
3. Taylor, W. R., and Green, M. (1989) *Eur. J. Biochem. 179*, 241−248.
4. Serrano, R. (1989) *Annu. Rev. Plant Physiol. Plant Mol. Biol. 40*, 61−94.
5. Schulz, G. E., Elzinga, M., Marx, F., and Schirmer, R. H. (1974) *Nature 250*, 120−123.
6. Clarke, D. M., Loo, T. W., and MacLennan, D. H. (1990) *J. Biol. Chem. 265*, 22223−22227.
7. Farley, R. A., Heart, E., Kabalin, M., Putnam, D., Wang, K., Kasho, V. N., and Faller, L. D. (1997) *Biochemistry 36*, 941−951.
8. Grisham, C. M., and Mildvan, A. S. (1974) *J. Biol. Chem. 249*, 3187−3197.
9. Grisham, C. M., and Mildvan, A. S. (1975) *J. Supramol. Struct. 3*, 304−313.
10. Kuriki, Y., Halsey, J., Biltonen, R., and Racker, E. (1976) *Biochemistry 15*, 4956−4961.
11. Askari, A., Huang, W.-H., and McCormick, P. W. (1983) *J. Biol. Chem. 258*, 3453−3460.
12. Jørgensen, P. L. (1974) *Biochim. Biophys. Acta 356*, 36−52.
13. Lowry, O. H., Rosenbrough, N. M., Farr, A. L., and Randall, R. J. (1951) *J. Biol. Chem. 193*, 265−275.
14. Hackney, D. D., Stempel, K. E., and Boyer, P. D. (1980) *Methods Enzymol. 64*, 60−83.
15. Smirnova, I. N., and Faller, L. D. (1993) *Biochemistry 32*, 5967−5977.
16. Smirnova, I. N., Lin, S.-H., & Faller, L. D. (1995) *Biochemistry 34*, 8657−8667.
17. Stempel, K. E., and Boyer, P. D. (1986) *Methods Enzymol. 126*, 618−639.
18. Boyer, P. D., de Meis, L., Carvalho, M. G. C., and Hackney, D. D. (1977) *Biochemistry 16*, 136−140.
19. Hackney, D. D. (1980) *J. Biol. Chem. 255*, 5320−5328.
20. Faller, L. D., and Diaz, R. A. (1989) *Biochemistry 28*, 6908−6914.
21. Altschul, S. F., Gish, W., Miller W., Myers, E. W., and Lipman, D. J. (1990) *J. Mol. Biol. 215*, 403−410.
22. Smirnova, I. N., Shestakov, A., S., Dubnova, E. B., and Baykov, A. A. (1989) *Eur. J. Biochem. 182*, 451−456.
23. Abele, U., and Schulz, G. E. (1995) *Protein Sci. 4*, 1262−1271.
24. Post, R. L., Toda, G., and Rogers, F. N. (1975) *J. Biol. Chem. 250*, 691−701.
25. Berberián, G., and Beaugé, L. (1991) in *The Sodium Pump: Recent Developments* (Kaplan, J. H., and De Weer, P., Eds.) pp 389−393, The Rockefeller University Press, New York.

26. Epstein, M., Kuriki, Y., Biltonen, R., and Racker, E. (1980) *Biochemistry 19*, 5564−5568.
27. Punzengruber, C., Prager, R., Kolassa, N., Winkler, F., and Suko, J. (1978) *Eur. J. Biochem. 92*, 349−359.
28. Kolassa, N., Punzengruber, C., Suko, J., and Makinose, M. (1979) *FEBS Lett. 108*, 495−500.
29. Dahms, A. S., and Boyer, P. D. (1973) *J. Biol. Chem. 248*, 3155−3162.
30. Glynn, I. M., and Karlish, S. J. D. (1990) *Annu. Rev. Biochem. 59*, 171−205.
31. Forbush, B., III (1987) *J. Biol. Chem. 262*, 11116−11127.
32. Babbitt, P. C., Hasson, M. S., Wedekind, J. E., Palmer, D. R. J., Barrett, W. C., Reed, G. H., Rayment, I., Ringe, D., Kenyon, G. L., and Gerlt, J. S. (1996) *Biochemistry 35*, 16489−16501.
33. Gerstein, M., Schulz, G., & Clothia, C. (1993) *J. Mol. Biol. 229*, 494−501.
34. Knowles, J. R. (1980) *Annu. Rev. Biochem. 49*, 877−919.
35. Richard, J. P., and Frey, P. A. (1978) *J. Am. Chem. Soc. 100*, 7757−7758.
36. Dahms, A. S., Kanazawa, T., and Boyer, P. D. (1973) *J. Biol. Chem. 248*, 6592−6595.
37. Cantley, L. C., Jr., Cantley, L. G., and Josephson, L. (1978) *J. Biol. Chem. 253*, 7361−7368.
38. Webb, M. R., and Trentham, D. R. (1981) *J. Biol. Chem. 256*, 4884−4887.
39. Xu, R-M., Carmel, G., Sweet, R. M., Kuret, J., and Cheng, X. (1995) *EMBO J. 14*, 1015−1023.
40. Wakabayshi, S., and Shigekawa, M. (1984) *J. Biol. Chem. 259*, 4427−4436.
41. Faller, L. E., Baroudy, B. M., Johnson, A. M., and Ewall, R. X. (1977) *Biochemistry 16*, 3864−3869.
42. Larsen, T. M., Wedekind, J. E., Rayment, I., and Reed, G. H. (1996) *Biochemistry 35*, 4349−4358.
43. Petsko, G. A., Kenyon, G. L., Gerlt, J. A., Ringe, D., and Kozarich, J. W. (1993) *Trends Biochem. Sci. 18*, 372−376.

BI970472Z